Dynamic Article Links ▶

PAPER

Pyridine as proton acceptor in the concerted proton electron transfer oxidation of phenol†

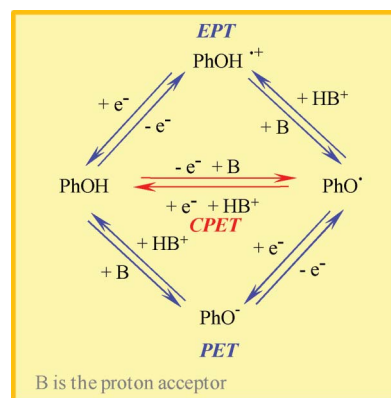**Julien Bonin, Cyrille Costentin, Marc Robert and Jean-Michel Savéant***

Taking pyridine as a prototypal example of biologically important nitrogen bases involved in proton-coupled electron transfers, it is shown with the example of the photochemically triggered oxidation of phenol by $Ru^{III}(bpy)_3$ that this proton acceptor partakes in a concerted pathway whose kinetic characteristics can be extracted from the overall kinetic response. The treatment of these data, implemented by the results of a parallel study carried out in heavy water, allowed the determination of the intrinsic kinetic characteristics of this proton acceptor. Comparison of the reorganization energies and of the pre-exponential factors previously derived for hydrogen phosphate and water (in water) as proton acceptors suggests that, in the case of pyridine, the proton charge is delocalized over a primary shell of water molecules firmly bound to the pyridinium cation.

Introduction

Homogeneous as well as heterogeneous oxidation of phenols has often been taken as a prototypal example in the mechanism analysis of proton coupled electron transfer (PCET) reactions,[1] an issue that attracts considerable current attention from a fundamental point of view and also in relation with the role of phenol oxidation in natural and artificial processes.[2]

One of the main thrusts of kinetic and mechanistic analysis of PCET reactions is to establish whether or not the reaction follows a concerted pathway (CPET) or one of the two stepwise pathways, PET (proton transfer first, followed by electron transfer) or EPT (electron transfer first, followed by proton transfer) as sketched in Scheme 1. Concerted processes indeed have the advantage of skipping high energy intermediates, and thus fully benefit from the increase of driving force deriving from protonation, provided the kinetic price that may have to be paid consequently is not too high.

We have recently examined in detail the intrinsic characteristics of water (in the solvent water) as opposed to those of a more conventional base, hydrogen phosphate, as proton acceptors in the photochemically triggered oxidation of phenol by $Ru^{III}(bpy)_3$.[3] The main conclusions reached then were as follows. Hydrogen phosphate is a more efficient proton acceptor simply because it offers a better driving force (7.2 in terms of *pH* units). However, when the intrinsic characteristics, *i.e.*, the characteristics

Laboratoire d'Electrochimie Moléculaire, UMR CNRS 7591, Université Paris Diderot, Bât. Lavoisier, 15 rue Jean-Antoine de Baif, 75205 Paris Cedex 13, France. E-mail: saveant@univ-paris-diderot.fr; Fax: +33 1 57 27 87 88; Tel: +33 1 57 27 87 95

† This work is dedicated to the memory of Athel Beckwith, a teacher and scientist from whom we learned how to study chemistry by example. His pioneering advances in radical chemistry laid the foundation for much of the current radical clock methodology.

Scheme 1

at zero-driving force are examined, water (in water) appears as a more efficient proton acceptor. The intrinsic characteristics are essentially the function of two parameters: the reorganization energy of the solvent resulting from the oxidative production of the proton and the pre-exponential factor, which reflects the coupling between the electronic states in the transition state and therefore the efficiency of proton transfer at this stage. The two parameters governing the intrinsic characteristics of water (in water) are both more favorable than in the case of phosphate. The reorganization energy is smaller, revealing that the proton charge is delocalized over a larger volume and the analysis of the pre-exponential factor indicates that the phenol–proton acceptor couple is flexible in line with a Grotthus-type mechanism for the delocalization of the charge over the hosting water cluster.

In this study, hydrogen phosphate was essentially used as a point of comparison to investigate the special character of water (in water) as a proton acceptor in a CPET reaction. The interest in

deriving the intrinsic properties of this particular proton acceptor also resides in the comparison with other proton acceptors, besides water, which may not only exert a different driving force but are chemically different so that one may expect different properties at zero driving force in terms of reorganization energies and pre-exponential factors. Among the various proton acceptors one may think of, a particular mention should be made of nitrogen bases in view of their ubiquitous role in natural processes. Their frequent involvement in H-bonded structures is a favorable factor for the occurrence of a CPET mechanism because the distance between the proton and the base corresponding to an H-bond is about the right distance for easy proton tunneling. As a representative of the family of H-bonding nitrogen bases, we selected pyridine as the proton acceptor for the present analysis of the kinetics of photochemically triggered oxidation of phenol by $Ru^{III}(bpy)_3$.

Results and discussion

Two series of laser flash experiments (see Experimental Section) were carried out. In the first series, the phenol oxidation second order rate constant was measured at a fixed temperature, namely 20 °C, as a function of the pyridine concentration at a pH (or pD) equal to the pK of pyridine both in light and heavy water (Fig. 1). As expected, raising the pyridine concentration results, after an initial plateau, in an increase of the pseudo-second order rate constant. It would seem that the variations in D_2O exhibit a shallow dip before the final rise of the rate constant. However, the scatter in the experimental data points ($\Delta \log k = 0.2$) is such that it does not allow one to consider this feature as significant.
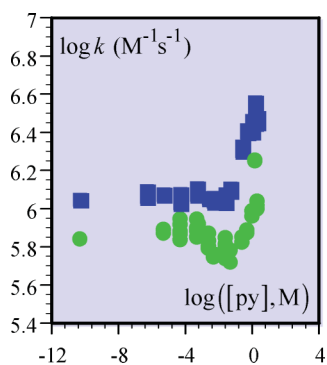
Fig. 1 Variation of the pseudo-second order phenol oxidation rate constant with the concentration of pyridine in equimolar solutions of pyridine and (H or D) pyridinium ion (see Experimental Section) at 20 °C, in light (squares) and heavy (circles) water. The left-hand data points were obtained in the absence of pyridine.

In another series of experiments, the temperature was varied at fixed values of the pyridine concentration both in light and heavy water (Fig. 2), at a pH (or pD) equal to the pK of pyridine both in light and heavy water.

As with phosphate,[3] the overall oxidation rate is the sum of three contributions, corresponding respectively to a concerted pathway in which the solvent, H_2O or D_2O, is the proton acceptor that we name H_2O (D_2O)-CPET, a "PET" pathway (see Scheme 1) in which OH^- is the proton acceptor, and—the object of the present study—a CPET pathway in which the purposely added base, here pyridine, functions as the proton acceptor (Py-CPET pathway).
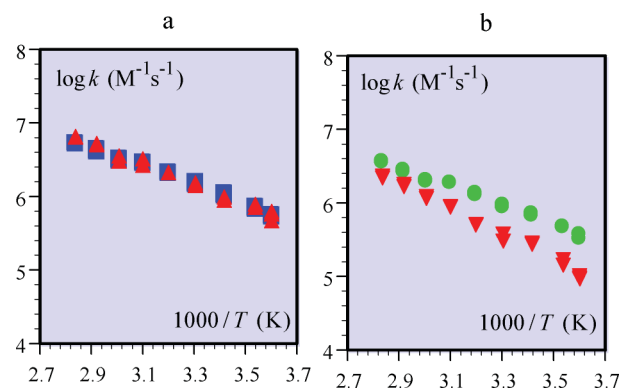
Fig. 2 Variation of the pseudo-second order phenol oxidation rate constant with temperature in 5×10^{-5} M equimolar solutions of pyridine and (H or D) pyridinium ion (see Experimental Section) at 20 °C, in light (squares in a, $pH = 5.4$) and heavy (circles in b, $pD = 5.7$) water compared with the variation of the pseudo-second order phenol oxidation rate constant with temperature in the absence of pyridine at $pH = 2$ (upward triangles in a) and $pD = 2.4$ (downward triangles in b).

At small concentrations of pyridine where the contribution of the Py-CPET pathway is deemed to be negligible, one expects that the rate constant should equal the value found in pure water for the water-CPET pathway, as for example the value found at pH 2. This is indeed the case with H_2O (Fig. 2a), indicating that at a pH equal to the pyridine pK in light water (5.2),[4] the OH^--PET pathway is not operating just because OH^- concentration is too low. The situation is different in D_2O (Fig. 2b) because the pyridine pK is higher (5.7),[4] opening a narrow but significant route for an OD^--PET pathway.
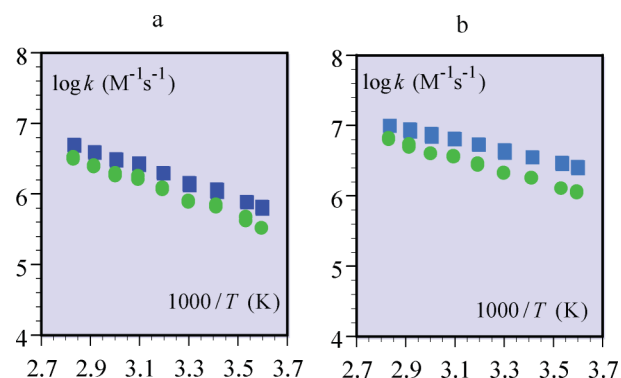
It is noted that this contribution increases upon going to lower temperatures, in line with a parallel increase of the pK in D_2O.[4]

It follows that the third-order rate constant for the Py-CPET pathway may be extracted from the raw data shown in Fig. 3 using eqn (1) in the case of H_2O:

$$k = k^H_{H_2O-CPET} + k^H_{Py-CPET}[Py] \qquad (1)$$

and eqn (2) in the case of D_2O:

$$k = k^D_{D_2O-CPET} + k_{OD^--PET} + k^D_{Py-CPET}[Py] \qquad (2)$$

Fig. 3 Variation of the pseudo-second order phenol oxidation rate constant with temperature in equimolar solutions of pyridine and (H or D) pyridinium ion (see Experimental Section) at 20 °C, in light (squares) and heavy (circles) water at fixed equal concentrations of pyridine and H- or D-pyridinium cation (M): 2.5×10^{-2} (a), 1.5 (b).

Thus leading to the Arrhenius plots displayed in Fig. 4, and finally to:

$$\ln\left(k_{Py-CPET}^{H}\right) = 18.1(\pm 0.05) - \frac{1105(\pm 15)}{T}$$

and:

$$\ln\left(k_{Py-CPET}^{D}\right) = 19.15(\pm 0.05) - \frac{1680(\pm 15)}{T}$$
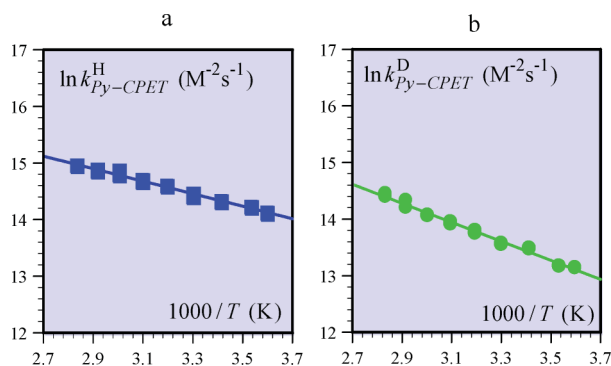
Fig. 4 a: Arrhenius plot for the third-order rate constant of the Py-CPET pathway in H_2O derived from the square-symbol data in Fig. 2 and 3 according to eqn (1). b: Arrhenius plot for the third-order rate constant of the Py-CPET pathway in D_2O derived from the circle-symbol data in Fig. 2 and 3 according to eqn (2).

Uncertainties are obtained from a statistical treatment of the data as detailed in reference 3.

These Arrhenius plots may be analyzed as follows in the same way as previously developed for hydrogen phosphate as the proton acceptor,[3] based on a model whose main features, summarized in Fig. 5, derive from a double application of the Born–Oppenheimer approximation. The transition state is defined by the intersection of the potential energy profiles of the reactant and product systems toward the heavy-atom coordinate (parabolae in Fig. 5). We may therefore start from a Marcus-type expression (eqn (3)) of the rate constant:

$$k = Z \exp\left[-\frac{w_R}{RT}\right]\exp\left[-\frac{\lambda}{4RT}\left(1 + \frac{\Delta G^0 - w_R + w_P}{\lambda}\right)^2\right] \quad (3)$$

Z is the pre-exponential factor. In the Franck–Condon exponential term, λ is the reorganization energy and ΔG^0, the reaction standard free energy. w_R and w_P are the work terms required to bring the reactants and products respectively, from infinite separation to reacting distance.

Arrhenius plots such as those in Fig. 4a and 4b are obtained by linearization of eqn (3) around the middle of the temperature range, T_m (313 K in our case). Although, Z and λ are the main terms in the expression of the Arrhenius intercept (I) and slope (S), respectively:

$$\ln k = I - \frac{S}{T}$$

other terms should also be taken into account. Both S and I contain three terms as listed in Table 1.

In the slope (equation (7) in Table 1), *reorg* is an increasing function of λ given by equation (9) in Table 1. The second
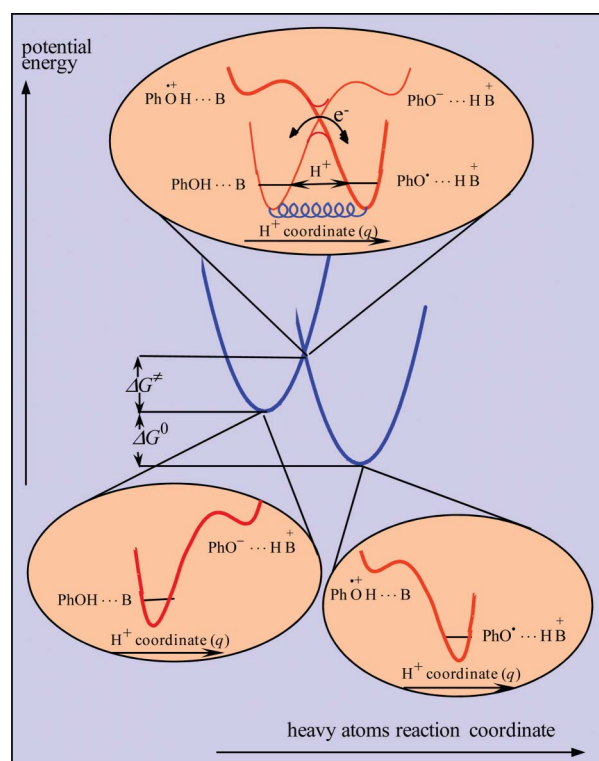
Fig. 5 Potential energy curves for the reorganization of the heavy atoms of the system, including solvent molecules (parabolae) and for the proton displacement concerted with electron transfer (upper insert). The symbols are defined in Scheme 1 and in the text.

term, *Stherm*, given by equation (10), contains the contributions of various thermodynamical parameters of the reactions and of work terms. The last term, *Sdyc* (equation (11)) derives from the dynamical coupling of the two states represented in the upper insert of Fig. 5: as sketched by the spring at the bottom of the barrier, proton tunneling is more efficient when the distance between the phenolic oxygen and the proton acceptor is smaller than its equilibrium value and *vice-versa*. *Sdyc* thus involves the force constant of the spring and the attenuation factor, β, of the exponential decay of the coupling of the two vibronic states with distance.

In the intercept (equation (8) in Table 1), the main term (equation (12)) is the value of the pre-exponential factor for the equilibrium distance between the phenolic oxygen and the proton acceptor, Z_{eq}. The term resulting from thermodynamics factors, *Itherm*, is given by equation (13). The dynamical coupling term, *Idyc*, (equation (14)) involves, as *Sdyc*, the force constant of the spring and the attenuation factor, β, of the exponential decay of the coupling of the two states with distance.

All ingredients of a full analysis of the reaction kinetics are gathered together in Table 1 so as to avoid browsing the whole paper in search of the pertinent equations and parameters.

The thermodynamic parameters necessary for the kinetic analysis were obtained from the following standard free energies and their variations with temperature:

$$\Delta G_{Py,H(D)}^{0,CPET} = \Delta G_{H_2O(D_2O)}^{0,CPET} - RT\ln 10\, pK^{Py,H(D)}$$

Table 1 Analysis of the thermodynamics and kinetics of the H_2O-CPET, PO_4H^{2-}-CPET and Py-CPET oxidation of phenol[g]

Parameters and equations			H_2O	PO_4H^{2-}	Py
Thermodynamics of the reaction:	$\Delta G^0 = -F(E^0_{Ru^{III}/Ru^{II}} - E^{0,CPET})$ $= \Delta H^0 - T\Delta S^0$	ΔH^0 (eV)	0.108 (H) 0.118 (D)	0.070 (H) 0.064 (D)	-0.066 (H) -0.060 (D)
		ΔS^0 (meV/K)	-0.072	1.228	0.38
		$\Delta G^0_{T_m}$ (eV) [a]	0.130 (H) 0.140 (D)	-0.311 (H) -0.317 (D)	-0.184 (H) -0.178 (D)
Work terms (assumed to be only from electrostatic origin) [b] and their variations with temperature: [c]	$w_{R \text{ or } P} = \dfrac{z_{R \text{ or } P}\, e_0^2}{4\pi\varepsilon_0\varepsilon_S d}$, $w_{R \text{ or } P} = \Delta H_{W_{R \text{ or } P}} - T\Delta S_{W_{R \text{ or } P}}$ $\Delta S_{W_{R \text{ or } P}} = -\dfrac{z_{R \text{ or } P} e_0^2}{4\pi\varepsilon_0 d}\dfrac{d}{dT}\left(\dfrac{1}{\varepsilon_S}\right)$ [c]	w_{R,T_m} (eV)	0	-0.171	0
		w_{P,T_m} (eV) [a]	0.057	-0.057	0.057
		ΔS_{W_R} (meV/K)	0	0.767	0
		ΔS_{W_P} (meV/K) [b]	-0.256	0.256	-0.256
		ΔH_{W_R} (eV)	0	0.069	0
$\Delta G^0_{T_m} - w_{R,T_m} + w_{P,T_m}$ (eV)			0.187 (H) 0.197 (D)	-0.197 (H) -0.203 (D)	-0.127 (H) -0.121 (D)
$\Delta S^0 - \Delta S_{W_R} + \Delta S_{W_P}$ (meV/K)			-0.322	0.717	0.124
$\lambda \left(= \dfrac{\lambda_{ox} + \lambda_{CPET}}{2}\right)$ [d] (16), λ_{CPET} (eV)			0.51±0.02, 0.45±0.04	0.72±0.02, 0.86±0.04	0.55±0.02, 0.53±0.04
$reorg = \dfrac{\lambda}{4R}\left(1 + \dfrac{\Delta G^0_{T_m} - w_{R,T_m} + w_{P,T_m}}{\lambda}\right)^2$ (K^{-1}) (9)			2765±50 (H) 2845±50 (D)	1100±50 (H) 1080±50 (D)	944±55 (H) 971±55 (D)
$Stherm = \dfrac{\Delta H_{W_R}}{R} + \dfrac{T_m}{2R}(\Delta S^0 - \Delta S_{W_R} + \Delta S_{W_P}) \times \left(1 + \dfrac{\Delta G^0_{T_m} - w_{R,T_m} + w_{P,T_m}}{\lambda}\right)$ (K^{-1}) (10)			-806±10 (H) -820±10 (D)	1740±10 (H) 1725±10 (D)	172±2 (H) 174±2 (D)
$Sdyc = \dfrac{2\beta^2 R T_m^2}{f}$ (K) [e] (11), $2R\dfrac{\beta^2}{f}$ (K^{-1})			1217±75, (H) 0.0125 ±0.001 1995±75, (D) 0.020 ±0.01	0, 0 (H) 620±80, (D) 0.0064±0.001	0, 0 (H) 500±70, (D) 0.006±0.001
Slope: $S = reorg + Stherm + Sdyc$ (K^{-1}) (7)			3175±15 (H) 4020±15 (D)	2830±15 (H) 3420±15 (D)	1105±15 (H) 1680±15 (D)
$\ln Z_{eq} = \ln\left\{\left[4\pi N_A \sigma^2 \sqrt{\langle \delta\sigma^2 \rangle}\sqrt{\pi/2}\right]\left[4\pi N_A r^2 \sqrt{\dfrac{RT}{f}}\sqrt{\pi/2}\right]\left[\dfrac{2}{\sqrt{\lambda}}\left(\dfrac{\pi}{RT}\right)^{\frac{3}{2}} C_{eq}^2\right]\nu_n\right\}$ (12) [e]			19.5±0.6 (H) 15.9±0.6 (D)	16.8±0.6 (H) 14.8±0.6 (D)	17.6±0.5 (H) 15.1±0.5 (D)
$Itherm = \dfrac{\Delta S_{W_R}}{R} + \dfrac{\Delta S^0 - \Delta S_{W_R} + \Delta S_{W_P}}{2R} \times \left(1 + \dfrac{\Delta G^0_{T_m} - w_{R,T_m} + w_{P,T_m}}{\lambda}\right)$ (13)			-2.60±0.03 (H) -2.64±0.03 (D)	11.90±0.03 (H) 11.90±0.03 (D)	0.55±0.03 (H) 0.56±0.03 (D)
$Idyc = \dfrac{4\beta^2 R T_m}{f}$ [f] (14)			7.8±0.5 (H) 6.3±0.5 (D)	0 (H) 4±0.5 (D)	0 (H) 3.5±0.5 (D)
$I = \ln Z_{eq} + Itherm + Idyc$ (8)			24.70±0.05 (H) 26.10±0.05 (D)	28.70±0.05 (H) 30.70±0.05 (D)	18.10±0.05 (H) 19.15±0.05 (D)
Variation with the driving force: $\ln(k) = \ln(Z_{eq}) + \left(\dfrac{2\beta^2 RT}{f} - \dfrac{w_R}{RT}\right) - \dfrac{\lambda}{4RT}\left(1 + \dfrac{\Delta G^0 - w_R + w_P}{\lambda}\right)^2$ (15)					

[a] $T_m = 313$ K. [b] approximating d, the distance between the two reactants (Scheme 2), by the value, 7 Å.[5] [c] $z_{R \text{ or } P}$ is the product of the charges in the reactant and product system respectively. ε_S, the solvent dielectric constant, varies with temperature: $d(1/\varepsilon_S)/dT = 6.213 \times 10^{-5}$ K^{-1}.[6] [d] λ_{ox}: self-exchange reorganization energy for the Ru$^{III/II}$ couple equated to 0.57 eV.[5] [e] for the definition of σ and r, see Scheme 2; $\sqrt{\langle \delta\sigma^2 \rangle}$: amplitude of the variation of σ; f: force constant of the harmonic oscillator of the H-bond between PhOH and B; C_{eq}: coupling constant between the two electronic states in the transition state at equilibrium distance between PhOH and B; ν_n: nuclear frequency. [f] β is the attenuation factor of the exponential decay of the coupling of the two states with distance. [g] Uncertainties are obtained from errors on the Arrhenius plots linear regression as detailed in reference 3 and assuming an uncertainty of 0.02 eV on the reorganization energy with pyridine.

where the first term, the standard free energy involved in the H₂O (D₂O)-CPET pathway, and its variations with temperature have been previously derived[3] and the second term is obtained from literature data recalled in Fig. 6.[4]
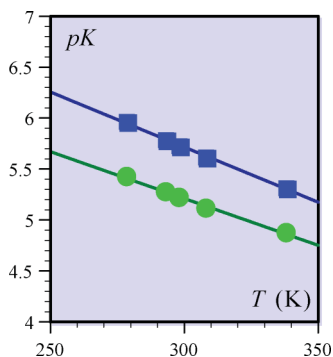

Fig. 6 Variation of the pyridine pKs in H$_2$O (squares) and D$_2$O (circles).

The work terms are assumed to be exclusively from electrostatic origin and to be the same in H$_2$O and D$_2$O. Their equivalent enthalpies and entropies are calculated according to the equations given in Table 1 where their values are also listed.

The treatment of data summarized in Table 1 was the same for parameter values listed in the last column of the Table. As discussed earlier,[3] the reorganization energy, λ_{CPET}, is mostly related to solvent reorganization, which can be grossly approximated by:[7]

$$\lambda_{CPET}^{(eV)} \approx \frac{3}{a(\text{Å})}$$

It follows that the solvation radius, a (see Scheme 2) is significantly larger for pyridine than for phosphate (approximately 5.7 Å *vs.* 3.5 Å). This observation suggests the involvement of a primary shell of water molecules, solidly bound to the pyridinium cation. A possible arrangement of these water molecules close to the *ortho* and *para* positions of pyridine is sketched in Scheme 2. The relatively small values found for the pre-exponential factor, Z, similar to those found for hydrogen phosphate and definitely smaller than for water, indeed fall in line with a strong association of these water molecules, in contrast with the Grotthus-type proton displacement taking place when water (in water) is the proton acceptor. This is also in agreement with the observation of a kinetic isotope effect independent of temperature.

Experimental

Ultrapure water (18.2 MΩ cm) from a MilliQ (Millipore) purification system or deuterium oxide (Euriso-Top, 99.9%) were employed to prepare the samples. Ru(bpy)₃Cl₂·6H₂O (Fluka, Technical Grade), phenol (Fluka, Ultra, ≥99.5%), pyridine (Fluka, ≥99.8%) were used without further purification. Methylviologen dichloride hydrate (Aldrich, 98%) was recrystallized from ethanol and dried overnight in vacuum before use.

The experimental setup used for the flash-quench measurements has been described previously in detail as well as the photophysics of the system.[8]

The transient absorption measurements were carried out with a laser flash photolysis spectrometer (Edinburgh Instruments, LP920-KS). The solutions were excited at 460 nm (5 ns pulse,
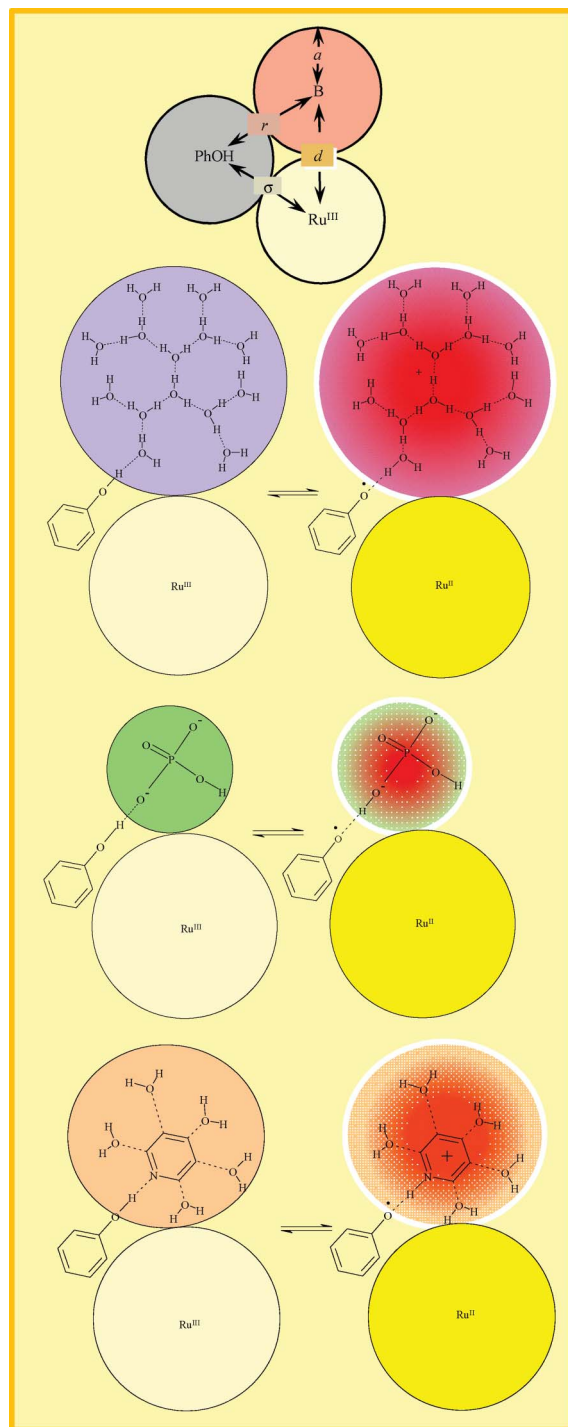
Scheme 2

6 to 8 mJ cm⁻²) *via* an OPO (Continuum, SLOPO Plus) pumped by a frequency-tripled Nd:YAG laser (Continuum, Surelite II-10). Perpendicular analyzing light provided by a 450 W ozone-free pulsed xenon lamp (Osram XBO) was collected into a spectrograph. Kinetics at 450 nm for Ru²⁺/Ru²⁺* and at 605 nm for MV•⁺ were then measured thanks to a photomultiplier tube (Hamamatsu, R928) linked to a 100 MHz oscilloscope (Tektronix, TDS 3012C). Samples typically contained 50 µM Ru complex, 40 mM MV²⁺, 25 mM phenol and different concentrations of

pyridine. Precise temperature of the sample port was set by a Peltier effect controller (Quantum Northwest TC125). The control and the synchronization of the whole setup were ensured by the Edinburgh Instruments L900 software.

The *pH* of the H_2O sample containing pyridine was adjusted at the value of the pyridine *pK* with concentrated HCl or NaOH and controlled with a Hanna, pH 210 pHmeter equipped with a microelectrode (6 mm, Bioblock Scientific) at 20 °C. The same was done in D_2O, the *pD* being obtained by adding 0.4 to the indication of the glass electrode.[9] Equimolar solutions of pyridine and (H or D) pyridinium ion could thus be obtained in this way both in H_2O and D_2O at 20 °C. The pyridine *pK* in H_2O changes with temperature,[4] but the *pH* and the *pK* remains practically equal. This also applies in D_2O.

All samples were purged with argon for 15 min prior to measurement.

Conclusions

Taking pyridine as a prototypal example of biologically important nitrogen bases involved in proton-coupled electron transfer, we have shown with the example of the photochemically triggered oxidation of phenol by $Ru^{III}(bpy)_3$ that this proton acceptor partakes in a concerted pathway whose kinetic characteristics can be extracted from the overall kinetic response. The treatment of these data, implemented by the results of a parallel study carried out in heavy water, allowed the determination of the intrinsic (*i.e.*

at zero driving force) kinetic characteristics of this proton acceptor in the same way as done previously with hydrogen phosphate and water (in water). Comparison of the reorganization energies and of the pre-exponential factors suggests that, in the case of pyridine, the proton charge is delocalized over a primary shell of water molecules firmly bound to the pyridinium cation.

Notes and references

1 *Chem. Rev.* special issue (number 12) on proton-coupled electron transfer, 2010, **110**.
2 C. Costentin, M. Robert and J.-M. Savéant, *Phys. Chem. Chem. Phys.*, 2010, **12**, 11179.
3 J. Bonin, C. Costentin, C. Louault, M. Robert and J.-M. Savéant, *J. Am. Chem. Soc.*, DOI: 10.1021/ja110935c.
4 I. R. Bellobono and P. Beltrame, *J. Chem. Soc. B*, 1969, 620.
5 N. Sutin and B. S. Brunschwig, *ACS Symp. Ser.*, 1982, **198**, 105.
6 *CRC Handbook of Chemistry and Physics*, 88th edn (ed. D. R. Lide) p. 6–3 (CRC Press, 2007).
7 J.-M. Savéant, *Elements of Molecular and Biomolecular Electrochemistry: An Electrochemical Approach to Electron Transfer Chemistry*; John Wiley & Sons: Hoboken, NJ, 2006. Chap. 1.
8 J. Bonin, C. Costentin, C. Louault, M. Robert, M. Routier and J.-M. Savéant, *Proc. Natl. Acad. Sci. U. S. A.*, 2010, **107**, 3367.
9 A. Krezel and W. Bal, *J. Inorg. Biochem.*, 2004, **98**, 161.

This journal is © The Royal Society of Chemistry 2011

Org. Biomol. Chem., 2011, **9**, 4064–4069 | 4069